The Astrophysical Journal, 770:26 (11pp), 2013 June 10 doi:10.1088/0004-637X/770/1/26

UBIQUITOUS NON-THERMALS IN ASTROPHYSICAL PLASMAS: RESTATING THE DIFFICULTY OF MAINTAINING MAXWELLIANS

J. D. Scudder[1] and H. Karimabadi[2]
[1] Department of Physics and Astronomy, University of Iowa, Iowa City, IA 54420, USA; jack-scudder@uiowa.edu
[2] SciberQuest, Del Mar, CA 92014, USA
Received 2013 February 23; accepted 2013 April 13; published 2013 May 21

ABSTRACT

This paper outlines the rather narrow conditions on a radiatively decoupled plasma where a Maxwell–Boltzmann (MB) distribution can be assumed with confidence. The complementary non-thermal distribution with non-perturbative kurtosis is argued to have a much broader purview than has previously been accepted. These conditions are expressed in terms of the electron Knudsen number, K_e, the ratio of the electron mean free path to the scale length of electron pressure. Rather generally, $f(v < v_2(K_e))$ will be Gaussian, so that MB atomic or wave particle effects controlled by speeds $v < v_2 \equiv w(15/8K_e)^{1/4}$ will remain defensible, where w is the most probable speed. The sufficient condition for Spitzer–Braginskii plasma fluid closure at the energy equation requires globally $K_e(s) \leqslant 0.01$; this *global* condition pertains to the maximum value of K_e along the arc length s of the magnetic field (to its extremities) provided that contiguous plasma remains uncoupled from the radiation field. The non-thermal regime $K_e > 0.01$ is common in all main-sequence stellar atmospheres above approximately 0.05 stellar radii from the surface. The entire solar corona and wind are included in this regime where non-thermal distributions with kurtosis are shown to be ubiquitous, heat flux is not well modeled by Spitzer–Braginskii closure, and fluid modeling is qualitative at best.

Key words: conduction – line: identification – plasmas – solar wind – stars: coronae

Online-only material: color figures

1. INTRODUCTION

A central assumption in studies of stellar atmospheres is that their velocity distribution functions (VDFs) $f(\mathbf{v})$ can be modeled reasonably well by a Maxwellian distribution, $f_{\rm MB}$. Three important examples that rely on this assumption are (1) the development for extended stellar atmospheres of closed fluid models, whose *existence* relies on the self-consistency of the Spitzer–Braginskii (SB) closure relations for a strongly magnetized plasma; (2) the inference of density and temperature information from emission line measurements; and (3) wave/turbulence normal mode determinations and their collisionless damping properties using the plasma dielectric.

If the Maxwellian assumption were no longer justified, it would have profound implications on the above studies. The construction of stellar atmosphere models and the chain of arguments leading to the conclusion that the observed thermal inversion of the corona requires a heating source are predicated on the validity of the SB closure model, and its suggestion that heat diverges from the temperature maximum flowing alternately toward the transition region and toward 1 AU. That surety would be withdrawn. The breakdown of the SB-based heat transfer model has the immediate consequence that the thermal inversion can no longer be equated to the need for a heat source, opening the door to alternative explanations. Generalizing the transport description implies that heat can sometimes flow up temperature gradients (Olbert 1983; Dorelli & Scudder 1999, 2003; Landi & Pantellini 2001), and be influenced by other gradients of fluid moments including the density and magnetic field strength (Scudder & Olbert 1983), possibly increasing the flow of heat into the regions where the corona is hottest. Preliminary work on these generalizations also shows that the determining factors for heat conduction may be distributed along the field line in a global way and have a decidedly different structure from Spitzer's local dependence on temperature gradient. Admitting that SB has collapsed implies that one cannot inventory the dominant process (conduction or waves) in setting the coronal temperature maximum while using the broken closure formalism.

For emission lines, the Maxwell–Boltzmann (MB) assumption allows detected lines and ratios of intensities to act as thermometers and assays of ambient density. The information in line spectra relies on modeling the rate integral over the distribution function times the known energy dependence of the atomic cross section. Without the MB assumption the lines become degenerate with a range of non-Maxwellian distributions; once the MB template is removed, the thermal–non-thermal degeneracy is compounded further for the ambiguity of what the most likely distribution function should be. Even the experimental inference that there are organized "turbulent" flows in the corona relies on interpretation of line profiles as if they must be Maxwellians, but widened in a self-similar way by the turbulent flow field. Most honest descriptions of turbulent broadening acknowledge it as a bandaid to fit the data (that could equally be ascribed to a non-thermal distribution; Scudder 1992). Alternatively, non-thermal interpretations of the excess width of line profiles would be allowed if Maxwellian postulates were not proscribed. Turbulent heating models of solar corona and associated wave damping studies rely heavily on the assumption of Maxwellian distributions. The identification of modes that can carry energy, rather than become evanescent, the quantitative size of non-resonant damping, and the vagaries of non-linear cascades that depend on which wave modes can propagate depend in general on $f(\mathbf{v})$ at all v and its moments, while the damping decrement depends on the slope of $\nabla_{\mathbf{v}} f(\mathbf{v})$ near the phase velocity. The Maxwellian VDF with its exponential dependence on energy predicts some modes to be evanescent, while they might be only lightly damped if a non-thermal tail

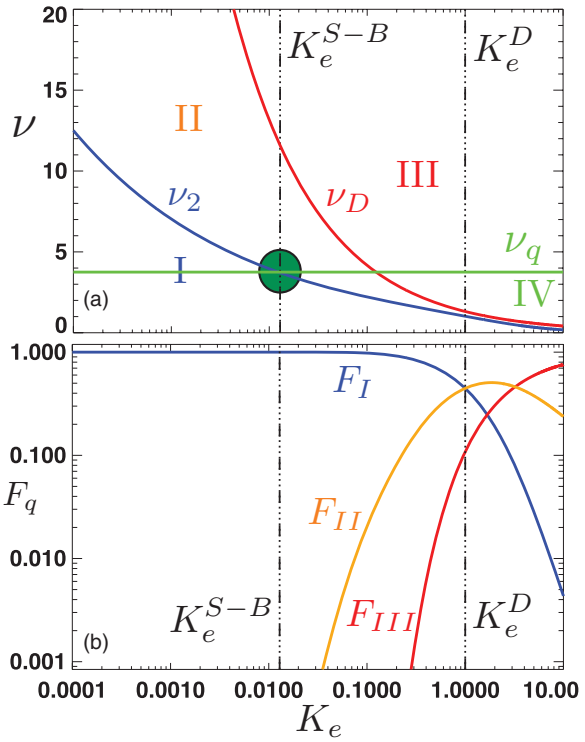

Figure 1. (a) Knudsen number variations for (1) ν_2 (blue), below which (Layer I) two or more collisions per scale take place; (2) ν_q (green), the minimum speed range (Layer IV) where SB closure scheme at the energy equation requires Coulomb effects sufficiently vigorous to keep $f(v \leqslant v_q)$ perturbatively close to a Maxwell–Boltzmann distribution; and (3) ν_D (red), the minimum speed driven into runaway (Layer III; discussed in Section 3). Knudsen numbers where $\nu_2(K_e) \geqslant \nu_q$ determine maximum Knudsen number, $K_e^* \simeq 0.01$ (green dot), where SB closure relation is self-consistent. Layer II is the complement of these definitions and resides between ν_2 and ν_D relationships. (b) Local density fraction F_j from the Layers I–III in panel (a).

(A color version of this figure is available in the online journal.)

were considered. A related point is that the number of resonant particles can be different with the non-thermal distribution, making the importance of damping or propagation based on MB assumptions increasingly problematic. The degree of the deviation from a Maxwellian that can be tolerated while deriving information remotely depends on the particular physics under consideration. Indeed, emission lines with different speed thresholds in the *same* plasma could be responding differentially to the non-thermal content present in the plasma if these thresholds straddled the thermal–suprathermal layer boundary ($\nu_2(K_e)$) we develop below in Figure 1.

Furthermore, we develop the perspective that the regime of the Maxwellian is a very narrow one in astrophysical plasmas, that is, supplanted by a more typical non-thermal distribution that has kurtosis that a Maxwellian does not have. This is shown by developing conditions for the validity of the Maxwellian assumption for these three important problems in stellar atmospheres. Remarkably, we find that the validity for the MB assumption is controlled by the size of a single parameter, the electron Knudsen number K_e, as shown in Figure 1. K_e is the electron mean free path divided by scale length of the gradients of the moments (we have chosen P_e to be specific) and is shown to be equal to another quantity of importance in plasma physics, the ratio of the parallel electric field to the Dreicer electric field.

We show here that there are three markers in velocity space controlled by K_e (Section 2; Figure 1(a)) that characterize the properties of the distribution function as they relate to transport models, dispersion properties, and sensitivity to atomic processes (e.g., impact ionization, recombination) for producing emission lines. In turn, these three markers allow a meaningful separation of the velocity space into thermal, non-thermal, and runaway "layers." Using these layers, three regimes of K_e are identified (Sections 2–4; Figure 1(b)) based on the relative density of electrons that occupies these three layers. In particular, the fluid closure founded on SB requires $K_e < 0.01$; even more disconcerting is the realization that not only must K_e be this small locally, it must be bounded across the entire system to which the modeled region is connected by the magnetic field where the plasma remains decoupled from the radiation field. We are then able to derive simple conditions (Section 3), relying only on parameters measurable from remote observations, to map out the regime of validity of the MB assumption for these problems of interest.

SB and the usual fluid treatment for a plasma is found to be self-consistent only if $K_e < 0.01$ globally, i.e., along the entire flux tube connected to the volume being modeled. As the first of several applications of this condition, we show in Section 4 that the main-sequence (MS) stellar atmospheres all violate this condition very low in their extended atmospheres and always below 0.05 stellar radii above the radius where the radiation field and plasma decouple. This regime, which includes the entire solar corona and wind for our Sun, is shown below to be the domain where non-thermal distributions should be ubiquitous, SB closure fails, and fluid modeling is *qualitative* at best. Interpretation of emission spectra based on the MB assumption are suggested (Section 3.2) to be most appropriate when the line's energy threshold speed $v*$ for the atomic physics (e.g., $(1/2)mv^{*2} = E^*$ at ionization threshold) satisfies the condition $v* < v_2(K_e)$.

Finally, dispersion and damping estimates based on MB shapes are found (Section 3.3) to be valid when the phase velocity or non-resonant interaction occurs below $v_2(K_e)$. In the VDF $f(v > v_2(Ke))$ non-thermal behavior is expected, *if this region is occupied*. Clearly, collisionless damping in these regimes will weaken with a shallower slope on $f(\mathbf{v})$, but will have more particles for resonance at phase speeds $v_\phi > v_2(K_e)$ than an MB of equivalent density and pressure.

Subsequently, we determine (Section 5) the radial profile of K_e for two recent models of stellar-solar wind atmospheres that reproduce the radial profiles of the solar atmosphere. Both solutions *locally* violate the consistency condition of SB. Both solutions violate the global requirement for SB self-consistency and also vacate the premise of their closure structure by using alternate heat laws for part of the radial domain assuming that the structure of the fluid equations remain unmodified. The two solutions compared also show $K_e > 0.01$ about 0.0023 stellar radii above the chromosphere, consistent with our modeling (Section 4), suggesting where the solar non-thermal transition should occur.

Since the issues of the self-consistency in the closure are most demanding when describing the electron heat flux, we concentrate on the collisional physics for electrons. We adopt the conventions of using the dimensionless velocity $\boldsymbol{\nu} \equiv (\mathbf{v}/w)$, where w is the thermal speed, which for a Maxwellian has the size $w = \sqrt{2kT/m}$, and using unsubscripted fluid variables for the electrons as in $T = T_e$, $m = m_e$, and $w = w_e$. As w is also the most probable speed of a Maxwellian, we use w as the most probable speed below when considering non-thermal distributions. Thus for the commonly used kappa

function $f(v) \propto (1 + (v^2/\kappa w^2))^{-(\kappa+1)}$, w will remain the most probable speed of that distribution, while its temperature $kT \equiv (P/n) = (\kappa m w^2/2\kappa - 3)$.

The remainder of this paper is organized as follows. Section 2 describes the development of the ideas and the derivation of the velocity space marker conditions for our proposed remote test of the MB approximation. Section 3 summarizes the results in easy form that can be used by to test the validity of fluid models or experimental interpretations of emission line observations or plasma dispersion estimates. Section 4 illustrates common properties of $K_e(r)$ model isothermal atmospheres along the MS of stellar evolution, showing that non-thermal physics is important in all MS stellar atmospheres outside of 0.05 stellar radii from the boundary where the plasma and radiation decouple. In Section 5, we apply our tests to the output of current solar wind fluid models determined from equations closed under the SB premise; both show that indeed the global condition $K_e < 0.01$ is violated low in the corona as predicted for MS stars. Summary and discussion follows in Section 6.

2. THE DERIVATION OF THE THREE SPEED MARKERS

In this section, we derive the three speed markers in velocity space that lead to the conditions for the validity of MB approximation. The first two markers v_q (Section 2.1) and v_2 (Section 2.2) arise from considerations of the SB model and Coulomb properties, whereas the third marker, v_D (Section 2.3), is based on the consideration of runaway physics, a phenomenon peculiar to scattering in plasmas. An overview of the suggested evolution of the lowest order distribution function as K_e increases is assembled in Section 2.4. We use Figure 1(a) to relate the analytical conditions that are being developed. At each K_e there are usually three intervals in v: Layer I *below* v_2 loosely termed the "thermals" in the following; Layer III *above* v_D loosely termed the "runaways" below; and Layer II sandwiched *between* the v_2 and v_D curves, referred to as the "non-thermals" below. As K_e increases, the width of Layers II and III change, with their lowest extremities trending down to smaller values of v. The next two sections establish from collisional theory the boundaries associated with v_q, v_2. The intersection (green circle) of the heat flux condition (the green line v_q) and the sufficient collisionality condition (blue curve v_2) determines the *allowable global maximum* Knudsen number K_e^* (blue vertical dashed line) where SB is self-consistent. As we proceed through this section, the other curves of this and the companion panel (Figure 1b) will shortly be integrated into the development.

The SB model aims to produce an accurate fluid description of the plasma for all moments up through the heat flux. SB is a perturbative model for correcting the local Maxwellian distribution to reflect weak, localized communication with its surroundings. Since there is no heat flow associated with a Maxwellian distribution, the heat flow in SB comes strictly from the perturbation δf. Thus the first condition for the validity of SB is that (i) $\delta f(v)/f_{\rm MB}(v) \ll 1$ over the range of velocities necessary to determine the heat flux, where v_q is determined as the finite upper limit of this range, given that its speed dependence is a given of the SB model. The second condition for the validity of SB is that (ii) there must be sufficiently vigorous collisions to keep $f(v < v_q)$ essentially Maxwellian. This leads to the second velocity marker $v_2(K_e)$, which is a function of the Knudsen number and is the upper boundary of the sphere in velocity space where self-Maxwellization is well under way, hence named the "thermals." The critical maximum size K_e^* where SB remains valid is determined by the last K_e where $v_2(K_e) \geqslant v_q$. This condition ensures that a Maxwellian will be a good zeroth-order estimate for the distribution function, and the heat flow moment will accurately be given by Spitzer's Fourier law form. Otherwise, SB closure collapses, the structure of the fluid equations for the plasma becomes unknown, and the heat law is not even qualitatively known.

2.1. SB and the Heat Flux Requirement: v_q

The mathematics of the SB method and the structure of the kinetic equation *dictate* the velocity space *dependence* of the corrections $\delta f(\mathbf{v}, \mathbf{x})$ to $f_{\rm MB}$ that support this weak gradient transport. In this approximation, δf takes on the separable form of

$$\delta f(\mathbf{v}, \mathbf{x}) = \alpha(x) f_{\rm MB}(v, \mathbf{x}) \sum_{j=0}^{2} \gamma_j(v) P_j(\cos\theta), \qquad (1)$$

where P_j is the jth Legendre polynomial. The only odd parity part of the perturbation, $\delta f_{\rm odd}(\mathbf{v})$, controls the parallel heat flux and possibly current; it is required to have the form

$$\delta f_{\rm odd}(v, \theta, \mathbf{x}) = \alpha(\mathbf{x}) f_{\rm MB}(v) \left(-\frac{5}{2}v + v^3\right) P_1(\cos\theta), \qquad (2)$$

where θ is the pitch angle of the particle. It is important for what follows to note that this perturbation is separable between $\mathbf{x}$ and $\mathbf{v}$ spaces since $\alpha(K_e(\mathbf{x}))$ controls all spatial dependence and the local strength of the heat flow through its Knudsen number dependence which is finally proportional to ∇T (Tanenbaum 1967), a circumstance that is only true for a lowest order MB distribution (Scudder & Olbert 1983).

The heat flux $q_\parallel$ is defined as the third moment of the distribution function; for a gyrotropic distribution function this takes the form

$$q_\parallel \equiv \frac{2}{\sqrt{\pi}} \int_0^\infty dv \int_{-1}^{1} d\cos\theta f(\mathbf{v}) \frac{1}{2} m w^3 v^5 P_1(\cos\theta) \qquad (3)$$

$$q_\parallel \equiv \int_0^\infty dv G_{q_\parallel}(v) = -\kappa(T)\hat{\mathbf{b}} \cdot \nabla T. \qquad (4)$$

Here κ is the thermal conductivity and Equation (4) restates Spitzer's familiar recovery of a Fourier's law form for heat conduction in a plasma. In Equation (4), the speed integrand has the form

$$G_{q_\parallel}(v) = \frac{\alpha(\mathbf{x}) 2nmw^3}{3\sqrt{\pi}} \exp(-v^2) \left(-\frac{5}{2}v^6 + v^8\right), \qquad (5)$$

shown in Figure 2 (black). Equations (4) and (5) are the result of the pitch angle integration for the heat flux, noting that $f_{\rm MB}$ has no angular dependence and thus supports no heat flux; the parts of δf that involve even Legendres do not contribute to the odd parity heat flux moment, since they are orthonormal to the P_1 weight of the heat flux moment on $[0, \pi]$.

Because $G_{q_\parallel}(v)$ changes sign under the integrand of Equation (4), it is difficult to estimate how the speed integral over $G_{q_\parallel}$ saturates to a final value. The self-consistency of the SB approach requires that this saturation occurs while the corrections in $\delta f(v)$ at different $\boldsymbol{v}$'s to $f_{\rm MB}(v)$ remain perturbative. Thus, the requirements are that (1) $\delta f(\boldsymbol{v})/f_{\rm MB}(v) \ll 1$, and that (2) the first condition is enforced for a range of speeds

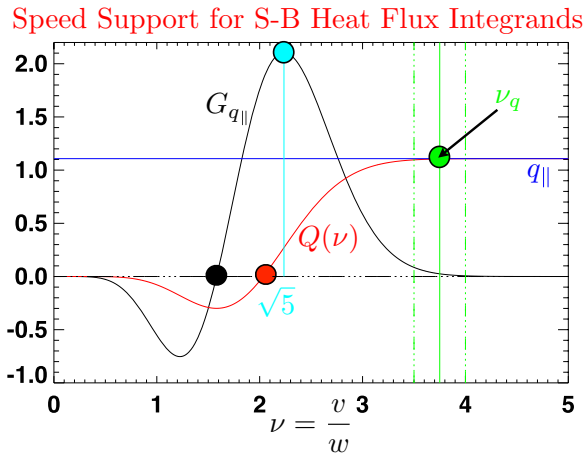

Figure 2. Dimensionless speed dependence of the integrand $G_{q_\parallel}(\nu)$ (ignoring units) for the heat flux moment (black), the partial heat flux integral $Q(\nu)$ (red) of the *illustrated* $G_{q_\parallel}(\nu')$ over the range $0 \leqslant \nu' \leqslant \nu$, and the total parallel heat flux $q_\parallel$ (blue). The convergence of $Q(\nu) \rightarrow q_\parallel$ defines ν_q (green dot, flanked by uncertainty indicated by vertical green dashed lines) as the upper limit of the minimum speed interval that must be dominated by Coulomb collisions for SB to be self-consistent.

(A color version of this figure is available in the online journal.)

$0 \leqslant \nu \leqslant \nu_q$ sufficiently broad to estimate the integral for $q_\parallel$ as the partial integral over the *finite* interval $[0, \nu_q]$, viz,

$$q_\parallel \simeq \int_0^{\nu_q} G_{q_\parallel}(\nu) d\nu. \tag{6}$$

Finding such a $\nu_q < \infty$ allows SB self-consistency at finite K_e outlined below (cf. Equation (13)). The possibility of this finite limit is connected to the dominance of the exponential in this integrand. Provided $\delta f(\nu)/f_{\rm MB}(\nu) \ll 1$ is only violated algebraically, i.e., weakly, such a looser requirement will allow the theory to make estimates in slight gradients.

Performing the indicated partial integration, the condition of Equation (6) becomes a search for the solution ν_q to this equation:

$$\begin{aligned} q_\parallel &\simeq Q(\nu_q) \\ &= \alpha(\mathbf{x}) \frac{nmw^3}{24\sqrt{\pi}} \left(e^{-\nu_q^2} \left(-30\nu_q - 20\nu_q^3 - 8\nu_q^5 - 8\nu_q^7 \right) \right. \\ &\quad \left. + 15\sqrt{\pi}\,\mathrm{Erf}(\nu_q) \right), \end{aligned} \tag{7}$$

which, in turn, becomes the search for when the exponential attenuation has won, viz,

$$e^{-\nu_q^2} \left(-30\nu_q - 20\nu_q^3 - 8\nu_q^5 - 8\nu_q^7 \right) \simeq 0. \tag{8}$$

The dimensionless dependence of $Q(\nu)$ is indicated in Figure 2 (red curve). From this figure, it becomes clear that the desired estimate for ν_q is conservatively where the red curve is no longer distinguishable from the horizontal blue curve at the value of $q_\parallel$. This condition is satisfied by the following inequality:

$$3.5 \leqslant \nu_q \leqslant 4.0. \tag{9}$$

The horizontal green line in Figure 1(a) reflects the SB *speed* condition of Equation (9) centered on $\langle \nu_q \rangle = 3.75$. Since the numerical range for ν_q is controlled by the speed dependence of the speed integrand of Equation (6), its size is unaffected by proportionality factors such as $\alpha(\mathbf{x})$, or the units of $G_{q_\parallel}$ as can be seen in Equation (8). The SB approach requires that collisions determine δf at least until $Q(\nu_q)$ saturates at the assumed closure value of the heat flux, $q_\parallel$. *If this condition is not enforced, the numerical value of the heat flux moment would increasingly and unphysically originate from parts of velocity space where* $f < 0$*; when this occurs at* $\hat{\mathbf{b}} \cdot \boldsymbol{\nu}_q < 0$*, it can appear to be making warranted contributions to the heat flux in spite of being kinetically unphysical. Alternately, these are circumstances where* $f(\mathbf{v}) = f_{\rm MB} + \delta f(\mathbf{v}) < 0$ *that are determining the integrated value of the moment and being ascribed to the medium via Fourier's (then) inappropriate use.*

If $\delta f(\nu \leqslant \nu_q)$ is maintained as a small correction compared to $f_{\rm MB}$ by Coulomb collisions, Maxwellians will be a good zeroth-order estimate for the distribution function, and the heat flow moment will accurately be given by Spitzer's Fourier law form. Otherwise, SB closure collapses (and the utility of the fluid equations) and the structure of the heat law is unknown.

2.2. Level of Collisions Required by SB: ν_2

But what level of collisionality is sufficient to keep $f(\nu \leqslant \nu_q)$ essentially Maxwellian? The Coulomb scattering is strongly speed dependent (unlike neutral scattering), a result that persists even after realistically describing the scattering of electrons from a large number of interacting protons with their Debye shielding electrons, and even in very strong magnetic fields (Montgomery et al. 1974).

The basic behavior is that the free path $\lambda(\nu)$ of an electron with speed ν relative to ion and electron target increases monotonically, *essentially* as the fourth power of ν:

$$\lambda(\nu) = \frac{4\sqrt{2}}{15} \lambda_{\rm mfp} \frac{\nu^4}{\mathscr{I}(\nu)}, \tag{10}$$

were $1 \leqslant \mathscr{I} \leqslant (3/2)$ is a slowly varying quantity (outlined in Appendix A), and the free path averaged over a Maxwellian distribution is indicated by the mean free path, $\lambda_{\rm mfp}$. Since Equation (10) (including the $\mathscr{I}$ dependence) is monotonically increasing, the *largest* speed ν_2 below which two or more scatterings occur per *shortest* gradient scale L (of the moments, e.g., n, $n\mathbf{U}$, P) is given by

$$2\lambda(\nu_2) = L, \tag{11}$$

where $L^{-1} = \max(d \ln \mathscr{M}/ds)$, where $\mathscr{M}$ are the moment quantities in the fluid equations and s is the arc length along the magnetic field. Using Equation (10) into Equation (11) determines the *inverse* Knudsen number scaling of the speed ν_2 to be

$$\nu_2(\nu, K_e) = \left(\frac{15\mathscr{I}(\nu)}{8\sqrt{2}K_e} \right)^{1/4}, \tag{12}$$

indicated by the *blue* curve in Figure 1(a). Since ν_2 measures the *upper* bounding speed (for fixed K_e) of the sphere in velocity space where collisions cause $f(\mathbf{v})$ to appear nearly Maxwellian, the clear consistency condition for the SB approach is that this ν_2 speed range of two or more collisions per L must *at least* be as large as ν_q, viz,

$$\nu_2(K_e) \geqslant \nu_q = 3.75 \pm 0.25. \tag{13}$$

Equation (13) implies that SB is self-consistent for all K_e where the blue curve in Figure 1(a) is *above* the green line. From

Equations (12) and (13), the condition and uncertainty for self-consistent SB closure and Maxwellian lowest order velocity distributions $f(v < v_2(K_e))$ becomes

$$K_e \leqslant K_e^* \equiv \frac{15\mathscr{I}(v_q)}{8\sqrt{2}{v_q}^4} \simeq 0.01 \pm 0.0026. \quad (14)$$

The estimated mean value of K_e^* is indicated by the dashed vertical blue line in Figures 1(a) and (b), set by the intersection at the green circle of the green and blue curves in Figure 1(a). This reasoning *for a plasma* yields results similar to, but perhaps more accessible than, earlier theoretical simulation, and experimental estimates (Gurevich & Istomin 1979; Gray & Kilkenny 1980; Scudder & Olbert 1983; Shoub 1983), but is well under the *neutral* Knudsen number regime, $K_n \leqslant 1$, found to be reasonable for describing laboratory transport in neutral gases.

Four nuances remain: (1) the SB condition is a global condition, requiring at the very least that $K_e(s) \leqslant K_e^*$ for all distances s along the magnetic tube of force piercing the local region of interest; (2) if globally $K_e < K_e^*$, then $f(v \leqslant 3.75, \mathbf{x}(s)) \simeq f_{\rm MB}(v)$ at all locales $\mathbf{x}(s)$ along the tube; if only locally $K_e(s) < K_e^*$, then there is no assurance that non-local contributions to $f(\boldsymbol{v})$) can be precluded; at best it suggests that $f(v \leqslant v_2(K_e) \simeq f_{\rm MB}(v \leqslant v_2)$. The misimpression remains in the literature (3) that SB consistency should be expected in a plasma up to Knudsen numbers of order unity (where neutral expansions seem to be satisfactory), despite Equation (14) and the literature cited above. Finally from Equation (14), it is now clear that had v_q been uncritically taken to be infinite, there would be no finite gradients in which SB would be self-consistent. As it is, the gradient regime where it is consistent is rather narrow, with $K_e \leqslant 0.01$.

When the SB fluid closure procedure is self-consistent, it is accompanied by a small *thermo-electric* field parallel to the magnetic field, $E_\parallel$, that counteracts the tendency of the plasma to conduct an electrical current when gradients cause heat to flow. While not present in thermodynamic equilibrium, $\epsilon \equiv (E_\parallel/E_D)$ is a perturbatively small, dimensionless quantity in the weak gradient SB description, where E_D is Dreicer's critical electric field discussed in the next section. ($E_\parallel$'s size was chosen by SB when determining the zero current form of Equation (1)). We now develop the role of ϵ as a bridge between the SB transport regime and the more commonly occurring astrophysical regimes where $K_e > K_e^*$.

2.3. Runaway Physics: v_D

Outside the SB framework, a conservation law connection between K_e and $E_\parallel$ exists in a plasma, which not only includes the expectation of a small thermo-electric $E_\parallel$ when $K_e \ll K_e^*$ but also provides interesting insight for regimes $K_e > K_e^*$ where SB fails. We first show that $\epsilon = K_e$ from conservation laws and then explore the impact of finite ϵ on the particle transport outside the SB regime.

The relation of the Knudsen number and the parallel electric field originates with the electron momentum equation:

$$E_\parallel \simeq -\frac{\hat{\mathbf{b}} \cdot \nabla \cdot P_e}{en_e}, \quad (15)$$

where the approximations involve neglecting the thermal force, gravitational, and inertial accelerations that are explicitly proportional to the electron mass. Comparing the parallel electric field of Equation (15) to Dreicer's electric field, E_D, (Dreicer 1959) defined by

$$eE_D\lambda_{\rm mfp} \equiv kT_e \quad (16)$$

yields the dimensionless electric field in Dreicer units, ϵ, defined by

$$\epsilon \equiv \frac{E_\parallel}{E_D} \simeq \lambda_{\rm mfp}\frac{d}{ds}\ln P_e \equiv K_e = \frac{\lambda_{\rm mfp}}{r}\frac{d\ln P_e}{d\ln r}\frac{dr}{ds}, \quad (17)$$

where the pressure tensor has been approximated as isotropic, s is the local coordinate along the magnetic field and the logarithmic derivative of the electron pressure determines the reciprocal of the local scale length, L. The mean free path in the definition of Dreicer's field (Equation (16)) is the electron scattering mean free path introduced previously. In the low corona, $(dr/ds) \simeq 1$.

Equation (17) is not a perturbative statement, so it may be used when K_e is not small. The content of Equation (17) *in the perturbative limit* was part of the original self-consistent SB approach (Spitzer 1962; Braginskii 1965) and accessible texts (Hazeltine & Waelbroeck 2004). The general transport regime $K_e \neq 0$ develops distributed electrical potentials to strive for quasi-neutrality and this relationship is a reflection of that cause and effect between gradients and $E_\parallel$, even when K_e is not perturbatively small.

Dreicer showed that *any* finite $E_\parallel$ divided velocity space into two volumes. The dividing surface is a paraboloid, cylindrically symmetric about the local magnetic field direction, with the minimum speed on this paraboloid called the Dreicer speed, v_D, occurring along the magnetic field along $\mathbf{F} = -eE_\parallel\hat{\mathbf{b}}$. For a given direction θ to $\mathbf{F}$, the paraboloid is denoted by $v_D(\theta) \geqslant v_D$. Outside this surface in velocity space (with apex at speed $v = v_D(K_e)$ indicated as Layer III in Figure 1(a)), electrons gain more energy from the plasma's parallel electric field, $E_\parallel$ (parallel acceleration), than they lose by collisions while traversing $\lambda_{\rm mfp}$. When populated this regime contains Dreicer's "runaways," which have no analog in neutral gas dynamics (Dreicer 1959, 1960; Fuchs et al. 1986). In velocity space, the parallel electric field promotes particles from underlying layers into runaway, producing a flux "into" local runaway. Historically, Dreicer phenomena have been associated with transient disruptions of laboratory plasmas, with electrons separating from the ions, hitting the vacuum walls, and terminating the experiment. There is, however, growing evidence that the parallel electric fields associated with gradients and needed to establish quasi-neutrality can also be "large" in the sense of Dreicer's modeling (Scudder 1996a, 1996b), but the resulting astrophysical system may nonetheless reach an equilibrium (Scudder & Olbert 1979), with runaways being recirculated on global scales much larger than $\lambda_{\rm mfp}$ because they cannot be localized with such strong fields. In this picture, the non-thermals and runaways at x_o are those recirculating runaways and non-thermals from "elsewhere" in the system that are passing through the immediate locale. Electrons in level II in Figure 1(a) are not quite runaways in the technical sense, but are particles with ranges for scattering greater than $\lambda_{\rm mfp}$ that increase as the v_D boundary is being approached and traversed. Thus, the strong electric field provides a natural recirculation across the levels of Figure 1(a).

Dreicer also showed that any finite $E_\parallel$ drives *some* particles into runaway. The *minimum* speed promoted into runaway,

denoted $v_D \leqslant v_D(\theta)$, is given by

$$v_D(K_e) \equiv \sqrt{\frac{3}{\epsilon}} = \sqrt{\frac{3}{K_e}}, \tag{18}$$

scaling *inversely* with $K_e^{1/2}$ as shown by the red curve in Figure 1(a). This speed forms the apex of the dividing paraboloid in velocity space. Its size and the variation of $v_D(\theta)$ control the fraction $F_{\rm III}$ of particles from a presumed MB distribution that would be driven into runaway. The K_e dependence of this fraction is shown by the red curve in Figure 1(b). In the SB regime $v_D(K_e) \gg v_2$, and this runaway fraction is presumed ignorable in the SB transport model (Spitzer 1962; Braginskii 1965). This tacit assumption forces one to reframe self-consistency of SB for astrophysics in the *global* form $K_e(s(\mathbf{x})) < K_e^*$ for all points s along the magnetic field linked to the volume of interest. At K_e^* where SB is locally last marginally self-consistent, $v_D(K_e^*) = 13.16$ (where the red curve crosses the vertical dashed blue line), more than nine thermal speeds above the v_q horizontal line for the SB heat flux description. While there *might* be *some* runaways in the SB valid regimes, they are assumed by SB to represent an inconsequential population with small corrections to $f(\boldsymbol{v})$ so they cannot impact the heat flux moment. If K_e^* is not a global bound along the magnetic flux tube connected to the volume of interest, there *could in principle* be particles above $v_D(K_e)$ that might influence the heat flow moment by their asymmetry. Note that Spitzer's treatment in the presence of the global bound on $K_e(s) \leqslant K_e^* = 0.01$ would not have such a regime. *The global weakness of gradients demanded by self-consistent SB closure preempts suprathermal physics from playing any role in heat flow in that description (Scudder & Olbert 1979)*. This circumstance reflects the limitation of the mathematics of the weak gradient expansion, not that non-thermals are irrelevant for heat conduction once violations like $K_e(s) > K_e^*$ occur on the tube of force.

2.4. Three Types of Electrons: The Mix of Kurtosis Increasing with K_e

In this section, we present the progression with K_e of the complexity of the electron distribution functions that can be anticipated from the three speed levels (I–III) discussed in Figure 1(a). In Figure 1(b), we have plotted the fractional density, F_j, of each of the layers versus K_e, on the assumption that the *local value* of K_e was the *uniform bound* on the flux tube. Colors in Figure 1(b) correspond to colors of roman numerals that identify levels in Figure 1(a). The velocity space volume for Layer I was assumed spherical with bounding radius v_2; the volume for Layer III was determined to be outside the paraboloid defined by Dreicer: $v = v_D(\theta)$ (Dreicer 1959); Layer II reflects the complementary volume, except that when $v_D < v_2$ we have set $v_2 = v_D$. This progression clearly emphasizes the increasingly "mixed" concentrations of different speed levels of Figure 1(a) in the distribution function that accompany $K_e > K_e^*$. The SB regime $K_e \leqslant K_e^*$ is the most collisional and hence Maxwellian regime (with very small kurtosis) with negligible parts of velocity space containing departures from MB behavior. As K_e increases, the collisional (level I) number fraction steadily decreases, and *kurtosis grows as a result*. The "thermal" level is no longer the majority constituent of the electrons when $K_e = K_D = 1$. Here the combined number fractions of levels II and III are equal partners with the level I density. Beyond $K_e \simeq 8$, level III electrons are the dominant determinants of the electron behavior, and the collisional level I electrons are entirely negligible. We show in Section 5 that the radial progression through $10^{-4} < K_e < 1$ occurs promptly within the first solar radius of the corona, leaving the clear impression that the corona is quickly permeated with non-thermal, kurtosis laden, electron distributions, as has been previously assumed (Scudder 1992).

Because the contributions of these three layers to the total electron density, number flux/current, pressure, and heat flux are all proportional to their number density, the progression of Figure 1(b) suggests the increasingly dominant roles of level II and III particles in any treatment that is attempted at the fluid level. Since these different levels will tend to have different effective mean energies, $\langle (1/2)v^2 \rangle_j$, the progression of Figure 1(b) suggests that these increasingly global particles will have more to say about the variation of pressure and temperature across these systems.

The existence of these three collisional classes with a varying density fraction allows for a rich mixture of ways to support the odd moments of current or heat flux. Because each level in velocity space experiences different forces across different scales, it is highly likely that they will contribute a different mean number fluxes, $nF_j\mathbf{U}_j = \langle \boldsymbol{v} \rangle_j$, and different partial contributions to the aggregate electron flux or heat flux. The net result, for the electron number flux

$$n\mathbf{U}_e = \sum_{j=\rm I}^{\rm III} \langle \boldsymbol{v} \rangle_j, \tag{19}$$

contains in general different velocity space levels (j) having different integrated contributions determined by their respective averages $\langle \ldots \rangle_j$. As the densities of all constituents are non-zero, the net result can hardly be surmised following the stochastic effects on only one of the components. Similarly, the heat flux for all the electrons,

$$q_{\parallel,e} = \frac{m}{2} \sum_{j=\rm I}^{\rm III} \langle |\boldsymbol{v} - \mathbf{U}|^2 \hat{\mathbf{b}} \cdot (\boldsymbol{v} - \mathbf{U}) \rangle_j, \tag{20}$$

will involve the factors that control the asymmetry of all three velocity space layers (in general) with different localizations.

In fact, the successful modeling of the interplanetary heat flux with two relatively drifting bi-Maxwellians for the core and halo (Feldman et al. 1975) is an example of this general type of contribution. The more loosely collisional halo population drifts away from the Sun in the ion rest frame, while the core lags behind the ion rest frame. This affords zero current, while having the heat flow controlled by the halo, in spite of only containing 10% of the density. The strahl could even be considered as the representative from level III, the runaways.

With these limited considerations it should be clear that the detailed SB collisional physics that describes heat flow ($K_e < K_e^*$) regime is increasingly supplanted by non-thermal physics as $K_e > K_e^*$. It is also clear that a quantitative transport theory has to respond to the possibility that a significant fraction of the particles are not locally thermalized by collisions. As this cannot be done in the SB framework, this must be viewed as an essential failure of that transport discussion. Since kurtosis is the first moment that inventories the number of such particles and it is missing in the SB closure, it must be included and allowed to be non-perturbative in any generalization of SB.

The Knudsen number variation with radius, $K_e(r)$, using solar wind data below (Figure 5), increases monotonically and rapidly

between 1 and 1.5 $R_\odot$ from (0.01–1); thus the horizontal axis of Figure 1(b) can be viewed as a radial progress of behavior to be expected in the lowest parts of the corona. The expected radial progression through higher values of $K_e(r)$ is very rapid (cf. Figure 5 below). With models below we show that this variation is nearly exponential at the base of the corona, placing the transport for the corona squarely *outside* the self-consistent SB regime essentially from the outset of the corona. As a reality check of this argument we note that $0.5 \leqslant K_e(1\ \mathrm{AU}) \leqslant 1$ and as this figure suggests, non-thermal halo and strahl particles (levels II and III) are routinely observed there (Feldman et al. 1975).

In reality, the local value of K_e may not be the uniform bound along the flux tube through this locale. This means that the segregation of levels I–III made on the basis of the local value of K_e will be modified for the non-locality this affords. When this happens, the level II and III particles found at r can, in principle, be "passing through" the surmised distribution function at r suggested when ignoring such non-local perturbations. *A transport theory for $K_e > 0.01$ is under development and will be reported elsewhere as it is outside the scope of this paper.* Without such a transport theory, it is difficult to provide much beyond these qualitative tendencies. Without such a transport description, it is impossible to judge the relative importance of wave-driven versus conduction-supported winds.

3. REMOTE TEST FOR THE VALIDITY OF THE MAXWELLIAN ASSUMPTION IN ASTROPHYSICAL PLASMAS

In this section, we integrate the results of Section 2 into simple conditions to map out the regime of validity of the MB assumption for these problems of interest.

3.1. SB and Heat Flow

When the magnetically linked plasma possesses Knudsen numbers that *globally* satisfy $K_e < 0.01$, accurate closure becomes possible with a heat flow essentially along **B** of the form $\mathbf{q}_\parallel = -\kappa(\partial T/\partial s)$. Without the *global* restriction such mathematical closure is impossible.

Proposed fluid solutions can be checked for global violations of $K_e < 0.01$ anywhere along the tubes of magnetic flux that thread the solution. If our examples below in Section 4 are representative, there are many fluid solutions whose gradients presume SB closure, but are not self-consistent with that closure. This evaluation can be determined after the solution is produced by exhibiting the variation of K_e obtained to show whether or not globally $K_e(s) \leqslant K_e^* = 0.01$. Model independent data of (n_e, T_e) from any source would be sufficient to calculate K_e and suggest the likely variation of non-thermals from the behavior of Figure 1(b).

3.2. Test for Emission Lines

The usual interpretation of emission lines assumes that the radiation originates in MB regimes. This approach can be retained for those emission lines whose energetic thresholds $\mathscr{E} = (1/2)mw^2v^{*2}$ have $v^* < v_2(K_e)$, where K_e is the Knudsen number in the source regime. We identify the layer of velocity space below $v^* \leqslant v_2(K_e)$ as acceptable (K_e, v) locales where emission spectra interpretations based on MB would appear justified for estimates of the thermal plasma present, whether SB is consistent or not. Layer I is the (K_e, v) region where MB-predicated emission line interpretations in terms of *thermal plasma* with thresholds $v^* \ll v_2(K_e)$ would be most secure regardless of SB consistency; the complementary union of regions II and III is the locale where non-thermal sensitivity is expected for emission lines with $v^* > v_2(K_e)$, and are regimes suitable for inferences of *non-thermal plasma* being present. Patterns of this type have been seen among lines formed from ions with varying ionization potentials, with those having higher ionization potentials seeming to require higher ambient temperatures than those with lower absolute ionization potentials (Bray et al. 2006).

It is possible that searches for non-thermal effects are not appropriately filtered for this effect. Alternately, it has been shown that the commonly observed enhanced line widths attributed to "turbulence" could also be signatures of non-thermal distributions in the source region (Scudder 1992). In this sense, the non-thermal signatures are being defined to be "turbulence" widths in an ad hoc way. When "turbulence" widths are suggested, a cursory consideration should be given to the likely size of K_e in the source region. Perhaps studies of "turbulence" widths could be inverted to see whether source regions where they are found are consistent with higher K_e values.

Typically non-thermal distributions observed in space are power laws at high energy. A commonly used distribution is Olbert's kappa function, (Olbert 1968) which has the form $f(v) = A(1 + (v^2/\kappa))^{-\kappa-1}$. Several observers are already reporting line profiles/ratios that require finite κ for electrons and/or ions (Dzifcáková et al. 2011; Lee et al. 2012), or more generally non-thermal distributions (Ko et al. 1996; Wilhelm et al. 1998; Pinfield et al. 1999; Esser & Edgar 2000). The expected line profile from kappa-induced Doppler broadening have been worked out and shown to organize the "turbulent" widths reported (Scudder 1992).

As an example of sensitivity to non-thermal distributions, the typical rate R of creation of a population that is a source of emission takes the form

$$R \propto 4\pi \int_{v^*}^{\infty} f(v)\sigma(v)v^3 dv \simeq 4\pi b f(v^*)\sigma(v^*)v^{*3}, \qquad (21)$$

where the second form suggests the control of R by $f(v^*)$ at the threshold for the atomic physics. Here, σ is the cross section for the process. In this approximation, Figure 3 demonstrates the strong rate enhancements possible with a kappa non-thermal distribution, rather than a thermal spectrum, of the same density and pressure. Very modest non-thermal distributions with $\kappa_e \simeq 20$ can have a 700-fold reaction rate enhancement that could make the difference between detection and not. For $\kappa_e \leqslant 7$, these enhancements can exceed 10^4. In the presence of non-thermals, many different combinations of non-thermal index and most probable speed can be the possible explanation for any given line's presence in spectra.

3.3. Test for Wave Damping

Modeling that incorporates collisionless damping calculations makes assumptions about the plasma distribution functions that control the plasma dielectric. The most likely regimes where the Maxwellian approximation for the plasma dielectric is possibly warranted are those *resonant* estimates that occur for phase velocities $v_\phi < v_2(K_e)$, and those non-resonant effects when the non-resonant particles principally occur below $v_2(K_e)$. Clearly, estimates of resonant damping for $v_\phi > v_2(K_e)$ using Maxwellian dielectrics are imprecise for the same reasons that the interpretation of emission lines would be for $v^* > v_2(K_e)$.

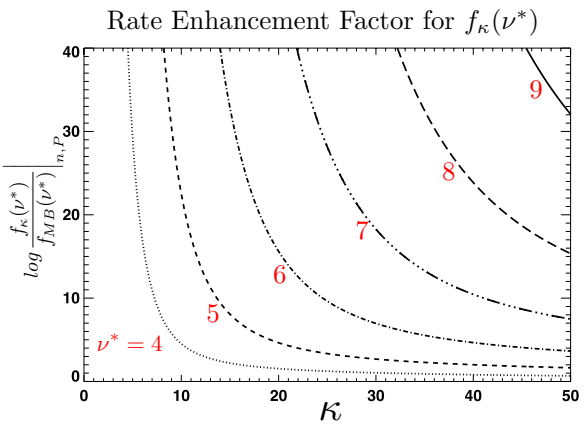

Figure 3. Variation at threshold, ν^*, of the ratio of phase space densities $f_\kappa(\nu^*)/f_{\rm MB}(\nu^*)$ as a function of ν^* and κ, where the compared f_κ and $f_{\rm MB}$ both have the *same* density and pressure, but different shape parameters. The importance of the non-thermal tail goes as κ^{-1}, with stronger tails at smaller κ and convergence to an MB distribution as $\kappa \to \infty$. Labeled curves are for a fixed threshold value (in red) of ν^* of the candidate reaction rate. When ν^* is in the suprathermal regime, strong enhancements are possible; these could make the difference between transitions being detectable in the presence of non-thermal distribution functions vs. below threshold in the presence of Maxwellians with the same density and pressure

(A color version of this figure is available in the online journal.)

4. VARIATION OF $K_e(r)$

Simple models of static isothermal atmospheres permit analytical estimates of the radial variation of the plasma Knudsen number, $K_e(r)$. The common density (Pannekoek 1922; Rosseland 1924) of electrons and ions is

$$n(r) = n_\circ \exp\left(-\beta_\circ\left(1 - \frac{r_\circ}{r}\right)\right), \tag{22}$$

where the large dimensionless constant $\beta_\circ = GM_\circ(M_p + m_e)/(2kT_\circ r_\circ)$ is the square of the escape divided by ion sound speeds at $r_\circ$. Stars on the MS have tightly bound atmospheres ensuring that $\beta_\circ$ is generally a large number. In Appendix B, theory and observations determine an MS range of $500 \leqslant \beta_\circ < 8000$, with the value for our Sun being $\beta_\odot \simeq 1925$ at a temperature of 5974 K.

The radial variation of the electron Knudsen number is determined by the variation of the mean free path $\lambda_{\rm mfp}(r)$ and the scale length of the isothermal pressure:

$$K_e(r) = \left|\lambda_{\rm mfp}(r)\frac{d\ln n_e}{dr}\right|. \tag{23}$$

With constant T, K_e becomes

$$K_e(r) = K_{e,\circ}\frac{r_\circ^2}{r^2}\exp\left(\beta_\circ\left(1 - \frac{r_\circ}{r}\right)\right), \tag{24}$$

where the base K_e is given by $K_{e\circ} \equiv \lambda_{\rm mfp}(r_\circ)\beta/r_\circ$. The base radius $r_\circ$ for the star should be a locale where the radiation and particle fields are essentially uncoupled. In the solar case we have taken this to be $r_\circ = R_\odot + 2080$ km in the chromosphere, where $T_{\rm o} \simeq 5974$ K.

We desire to invert Equation (24) to obtain $r(K_e)$ and from it where in the atmosphere $K_e^* = 0.01$ occurs. Given the strong exponential dependence of Equation (24), $r(K_e(r))$ is determined perturbatively in terms of $\Delta r = r - r_\circ$; after assuming

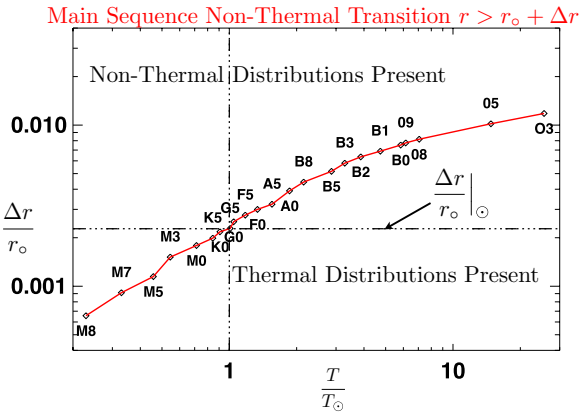

Figure 4. Estimates of the variation (red) across main-sequence stars of the heights $\Delta r/r_\circ$, where transition to suprathermal signatures occurs, vs. photospheric temperature relative to the Sun, $T/T_\odot$. The radius where the plasma becomes uncoupled from the radiation field is denoted as $r_\circ$. The altitude Δr of this transition to significantly suprathermal $f(\boldsymbol{v})$ is suggested (red curve) for M8–O3 stars to be between 0.00065 and 0.013 $r_\circ$ above $r_\circ$. Non-thermal distributions are expected above the red curve; thermal spectra are expected below the red curve. Above the red curve, Spitzer–Braginksii transport coefficients are not theoretically defensible.

(A color version of this figure is available in the online journal.)

$\Delta r \ll r_\circ$, we obtain the approximate form

$$\frac{\Delta r}{r_\circ} \simeq \frac{\ln\frac{K_e(r)}{K_{e\circ}}}{\beta_\circ - 2}. \tag{25}$$

Assuming $K_{e\circ} \simeq 10^{-4}$ (Fontenla et al. 1990), we now estimate $\Delta r(K_e^*)$ above which non-thermal signatures are expected and SB closure fails. This result depends only logarithmically on the poorly known base Knudsen number, $K_{e,\circ}$, that we have estimated based on solar modeling. To qualify our result by this ambiguity, we incorporate the statement of our assumption

$$\frac{\Delta r}{r_\circ} \simeq \frac{4.6 + 2.3\log\frac{10^{-4}}{K_{e\circ}}}{\beta_\circ}, \tag{26}$$

where non-thermal distributions should be expected and common logarithms are used. The large value of $\beta_\circ$ controls the size of this result despite the ambiguity of the base Knudsen number. Equation (25) would only be increased five fold to $23/\beta_\circ$ on the assumption that $K_{e\circ} = 10^{-12}$. Across the entire MS, the non-thermal transition occurs very low in the atmosphere, ranging (red curve in Figure 4) from $0.00065 \leqslant (\Delta r/r_*)|_{\rm MS} \leqslant 0.013$, centered on the solar value of $(\Delta r/r_\circ)|_\odot \simeq 0.0023$. Considering the extreme ambiguities in $K_{e\circ}$, these estimates might be low by a factor of five, but are certainly less than 0.01 for the Sun, and below 0.004–0.05 across the MS stars in Figure 4.

For the Sun, this implies that within 1600 km above the base height of $r_\circ \simeq R_\odot + 2080$ km, *non-thermal physics should be a part of the solar atmosphere and SB transport no longer valid.* Because large $\beta_\circ$ is the hallmark of MS stars, the *radially precipitous transition to ubiquitous non-thermal distributions is a general expectation for all MS stars*. This conclusion links the existence of suprathermal parts of $f(v)$ to gravity, the Rutherford cross section, and gradients of the equilibrium moment profiles, rather than (1) instability thresholds, (2) posited power spectra of turbulence, or (3) other forms of time dependence as the agent for promotion of the particles to form the suprathermal tails.

While such simple models may not completely reproduce profiles of the entire atmosphere, these calculations suggest

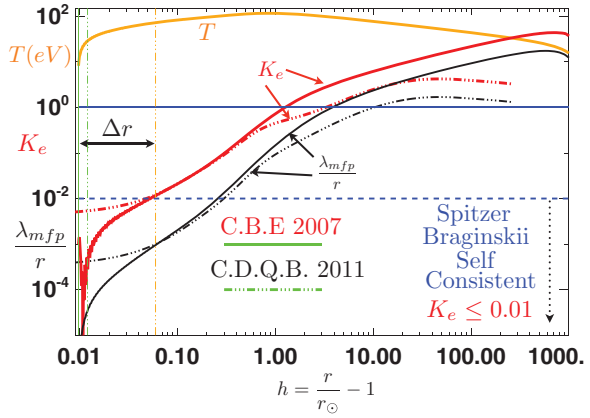

Figure 5. Variation of Knudsen number, K_e (red solid curve, CBE; red dashed curve, CDQB), from two wave-driven solar wind solutions that include SB heat conduction at small radii before switching over to saturated heat flux (Hollweg 1974); variation of λ_{mfp}/r (black dashed curve, CDQB; black solid curve, CBE). Upper bound for self-consistent Spitzer–Braginskii regime is the blue dashed line ($K_e < 0.01$). Vertical line at Δr illustrates where the current paper predicts where the solar Knudsen number should exceed SB threshold, $K_e > 0.01$.

(A color version of this figure is available in the online journal.)

that K_e does initially rise precipitously when the atmosphere is fully ionized (cf. Figure 5, below), making suprathermal physics important, if not controlling, in the lowest reaches of these atmospheres, *within a few hundredths of the base radius*.

5. $K_e(r)$ IN WAVE-DRIVEN SOLAR WIND MODELS

Fluid solutions are often used to evaluate the consequences of various forms of energy addition to the solar wind (Chandran et al. 2011, hereafter CDQB; Cranmer et al. 2007, hereafter CBE). Both CDQB and CBE model an Alfvén-wave-driven wind and both use a two-zone model for the heat flux (Hollweg 1974), with SB closure assumed below $r*$ (where $2\lambda_{\rm mfp}(r*)/r* \simeq 1$) smoothly joins Hollweg's saturated model beyond. The CDQB model contains two fluids with proton anisotropy, while CBE is a one-fluid treatment. The one-fluid model starts at the photosphere, while the two-fluid solution starts from an inner boundary condition essentially at 1.01 $R_\odot$. The structure of the one-fluid equations is set by SB closure projections, but has additional source and sink terms associated with the modeled wave dissipation considered. The two-fluid model uses a fluid structure set by SB closure for the electrons and a closure for the ions modified for bi-Maxwellians, but not for closure impacts due to waves.

Figure 5 summarizes the radial variation of $\lambda_{\rm mfp}/r$ for these solutions (black solid curve, CBE; black dashed curve, CDQB), together with the radial variation of the electron Knudsen number (red solid curve, CBE; red dashed curve, CDQB) determined using the identity

$$K_e \equiv \frac{\partial \ln P_e}{\partial \ln r} \frac{\lambda_{\rm mfp}}{r} \frac{dr}{ds}. \quad (27)$$

The horizontal blue dashed line is the maximum Knudsen number $K_e^* = 0.01$ for which SB transport and closure is self-consistent. Beyond $h = 0.05$, both fluid solution profiles *exceed* the maximum $K_e^* = 0.01$ threshold for self-consistent SB closure. This is approximately the maximum location Δr estimated in Section 3 where $K_e(r) > 0.01$ was to be expected in the solar case. Additionally, the solutions both have $K_e(r)$ profiles that rapidly increase with r (like the theoretical solutions in Section 3), exceeding $K_e \simeq 1$ in the vicinity of $h \simeq 1$, and rising still further until turning over beyond $h \simeq 10$. The CDQB solutions infer that the Alfvén wave energy flux is deposited within $h \simeq 10$, across the same interval where the SB description of the heat flow is inconsistent with the $K_e > 0.01$ limit for self-consistency. The coronal temperature maximum occurs near $h = 1$, in the middle of the interval where the Alfvén wave energy is suggested to dissipate and where the heat flow used in the equations is inconsistently described by the SB formula.

This retrospective analysis of these solutions raises several questions. If SB is not self-consistently affirmed, as here, what equations describe the plasma at the fluid level? Is the implied parallel electric field of such a model consistent? It is the ultimate microscopic force that accelerates the wind. What is the implication of integrating the fluid equations, with electrons closed using the SB approach, using an incorrect heat flux and inferring that an additional energy source is required? The situation for the energy equation is different than the one-fluid continuity and momentum equations, where summational invariants ordain the vanishing of collisional contributions to the equations. However, a similar complication is in play for the two-fluid description, even at the momentum level via the thermal force. Can the argument be pursued that such equations with such liabilities nonetheless affirm the wave-driven scenario for the wind's acceleration? Can the inadequacies of conduction to drive the wind really be adduced when its description and closure framework are so much in question? These are but a few of the questions that our finding opens for careful further consideration. These considerations will be undertaken elsewhere, as will our approach to extending the SB closure with a different macroscopic approach.

On the surface, it would appear difficult to address the pressing problem of the coronal temperature inversion by including new effects in a fluid description that simultaneously has a flawed description of the heat flux that if described appropriately might potentially be competitive for explaining the temperature inversion of the corona.

6. CONCLUSIONS AND DISCUSSION

The conditions for expecting an MB distribution in an astrophysical plasma are restricted to magnetically linked volumes of plasma whose $K_e(s)$ are globally below $K_e^* \equiv 0.01$. In the heavily bound atmospheres of MS stars, the transition away from MB distributions occurs rather low, less than $\Delta r \simeq 0.01$–$0.05 r_\circ$ above $r_\circ$ which is the height in the atmosphere where the radiation field and the particles are decoupled. Non-thermal plasma distributions in the fully ionized atmospheres of MS stars should be commonplace above these heights. In isothermal atmospheres the Knudsen number grows radially outward, initially exponentially. Two recent solar wind solutions that reproduce observations illustrate strong growth of K_e with increasing r, and both show that the above estimate where the Knudsen number in the atmosphere passes through 0.01 is as predicted from our analysis in Section 4 above.

The solutions and observations suggest that the electron Knudsen number continues to grow with increasing radius, exceeding $K_e \simeq 1$ before the temperature maxima seen in the same solutions. We have shown in Figure 1(b) that there is every expectation that non-thermal distributions will accompany this growth of $K_e > 0.01$. It is known at 1 AU where $0.5 < K_e < 1$ that the observed ambient $f(\mathbf{v})$ is decidedly non-thermal just as our general arguments have suggested.

We have also seen that the very small and restricted domain for SB closure is also the same regime where non-thermals have a negligible presence (cf. Figure 1(b)). We have suggested that the proscribed absence of non-thermals required for the self-consistency of SB is also why it cannot work for astrophysics, since the non-thermals are almost impossible to avoid, being inherently related to gravity, the energy dependence of the Coulomb cross section, expansion into essentially a vacuum, and the deep connection between K_e and $\epsilon = (E_\parallel/E_D)$. The extensions of stellar atmospheres with their rapidly depleted densities develop space charge problems that produce $E_\parallel$ for equilibrium that require variations of K_e to support that equilibrium. With increasing K_e come the non-thermals; with the non-thermals comes non-perturbative kurtosis that is not allowed in the SB framework. We have argued that more general closures of the type Grad has suggested will be required for the astrophysical regimes; these closures should consider lowest order distributions with kurtosis variation. Such new closures will have energy and new "fluid" equations that are structurally different from those obtained assuming SB closure and lowest order Maxwellian distribution functions. At the very least such new equations must keep track of kurtosis and the variation of kurtosis in its moment level analysis.

The suggested generality of non-thermal distributions provides a way to understand how the predictions of an approach like velocity filtration can be involved in understanding the inversion of MS coronae. The velocity filtration model (Scudder 1992) for understanding the temperature inversions of MS coronae essentially followed a model kinetic equation in which the initial conditions had kurtosis. In the collisionless Vlasov limit, the kurtosis of a kappa function is invariant across retarding potentials, but has other interesting properties such as density and temperature anti-correlated. This behavior was outside what SB could produce and it was outside the approximations of polytropic closure. But that calculation is precisely what transport would permit in the infinite K_e regime and its basic features have been documented even with the inclusion of Coulomb collisions in Fokker–Planck codes (Dorelli & Scudder 2003) and modern exospheric solutions (Pierrard & Lazar 2010). To be sure, pure velocity filtration is not the appropriate description for *all* the different speed layers of Figure 1(a) that we have discussed here, but it is the dominant effect on the pressure when the gas is climbing out of a deep stellar centered gravitational trap. It is no accident that all MS stars have these temperature inversions, and they all have the tightly bound atmospheres of Section 4 with the large β values. This circumstance assures us that the velocity filtration effect, enabled by kurtosis, has a large impact on the temperature profiles of these stars, including being able to produce their inverted profiles.

Strong sensitivity of emission lines and collisionless damping signatures were shown when threshold energies or phase velocity energies occur in the suprathermal parts of velocity space with electron kinetic energy thresholds $E > \sqrt{(15/8K_e)}kT_e*$, where $T_e* = (2\kappa_e - 3/2\kappa_e)T_e < T_e$, where T_e is the total random energy for the electrons and $1.5 < \kappa \leqslant \infty$.

Second, the transport models of Spitzer and Braginskii are clearly contraindicated when $K_e > 0.01$ occurs along any part of the magnetically linked regions to the volume of interest. Non-thermals are suggested to become generally important in MS atmospheres, either from local production above $\Delta r/r_\circ = 0.01$ or from non-local transport from regions away from the volume of interest. It is a very difficult research problem to assure that any given region should have a Maxwellian distribution when magnetically linked to other regions where strong runaways are produced.

Third, the significant kurtosis implied by these non-thermal populations militates for the exploration of more general closures (Grad 1949) that are not so closely tied to thermal states of local thermodynamic equilibrium as those used by Spitzer and Braginskii which have no kurtosis. There are already interesting aspects of this type of description capable of producing the coronal temperature profile in the collisionless ($K_e = \infty$) limit (Scudder 1992) and explaining the Helios solar wind proton distribution functions (Leblanc & Hubert 1998). Making allowance for non-perturbative kurtosis (as is possible by Grad's method) seems to be the essential next step toward an astrophysically useful transport theory that would eventually predict the skew of that kurtotic component on a coequal basis with the other lower moments and not presume to produce the skew and kurtosis perturbatively as the SB expansions do.

We acknowledge grant support from NSF 1202152, discussions with and data for Figure 5 from B. D. Chandran and S. R. Cranmer, together with manuscript comments from P. Cargill, D.A. Roberts, E. Lee, and R.E. Hartle.

APPENDIX A

SPEED DEPENDENCE OF λ (ν) FOR ELECTRON SCATTERING: EQUATION (10)

Electron scattering in the plasma occurs off of ions with ν_{ei} as well as off of background electrons with ν_{ee}. Assuming that electrons and ions have the same kinetic temperature T, their velocity distributions have thermal speeds that differ by $\sqrt{(M/m)} \simeq 42$. As usual, collision rates add and the scattering rate for relative speed ν, which is dimensionless in electron thermal speed variables, involves the number of scatterers with speed below that of the relative speed. The number of such protons, $\delta n_+(\nu)$, and electrons, $\delta n_-(\nu)$, are given by the expressions

$$\delta n_+(\nu) = \frac{4n}{\sqrt{\pi}} \int_0^\nu \exp\left(-\frac{M}{m}\nu'^2\right)\left(\frac{M}{m}\right)^{3/2} \nu'^2 d\nu' \qquad \text{(A1)}$$

and

$$\delta n_- = \frac{4n}{\sqrt{\pi}} \int_0^\nu \exp(-\nu'^2)\nu'^2 d\nu'. \qquad \text{(A2)}$$

The total electron Coulomb collision frequency $\omega_e(\nu)$ for relative speed ν becomes

$$\omega_e(\nu) = \alpha \frac{\delta n_+(\nu) + \delta n_-(\nu)/2}{\nu^3}, \qquad \text{(A3)}$$

where the factor of one-half originates in the reduced mass for e–e scattering, and the inverse cubic dependence is from the Rutherford behavior for the Coulomb interaction. In turn, the free path for relative speed ν is given by

$$\lambda(\nu) = \frac{\nu}{\omega_e} = \frac{1}{n\alpha}\frac{\nu^4}{\mathscr{I}(\nu)}, \qquad \text{(A4)}$$

where

$$\mathscr{I}(\nu) \equiv \left(\mathrm{Erf}\left[\sqrt{\frac{M}{m}}\nu\right] + \frac{1}{2}\mathrm{Erf}[\nu] - \frac{\nu}{\sqrt{\pi}}\left(2\sqrt{\frac{M}{m}}\exp\left[-\frac{M}{m}\nu^2\right] + \exp[-\nu^2]\right)\right). \qquad \text{(A5)}$$

The full speed dependence of $\mathscr{I}$ has three zones with slightly different structures: (1) $\nu < 1/42$, (2) $1/42 < \nu < 1$, and (3) $\nu > 1$, where $\mathscr{I}$ may be successively approximated as

$$\mathscr{I}\left(\nu \ll \sqrt{\frac{m}{M}}\right) \simeq \frac{4}{3\sqrt{\pi}}\nu^3\left(\left(\frac{M}{m}\right)^{3/2}+1\right), \quad \text{(A6)}$$

or

$$\mathscr{I}\left(\sqrt{\frac{m}{M}} < \nu < 1\right) \simeq 1+\mathrm{Erf}(\nu)/2-\nu\exp(-\nu^2)/\sqrt{\pi}, \quad \text{(A7)}$$

or

$$\mathscr{I}(1 \ll \nu) \simeq 3/2. \quad \text{(A8)}$$

Because there are so few electrons in the first regime, its functional dependence hardly influences the mean free path; the other two regions do however; there $\mathscr{I}$ is of order unity and weakly varying. This leaves the basic speed dependence across essentially the total electron spectrum as $\lambda(\nu) \propto \nu^4$ as we have used in Equation (10). Between approximations of Equations (A7) and (A8) $1 \leqslant \mathscr{I}(\nu) \leqslant 3/2$, which causes a slightly different normalization when extracting the actual mean free path λ_{mfp} in front of the accurate speed dependence, viz,

$$\lambda_{\mathrm{accurate}}(\nu) = 0.3770\lambda_{\mathrm{mfp}}\frac{\nu^4}{\mathscr{I}(\nu)} \simeq \frac{4\sqrt{2}}{15}\lambda_{\mathrm{mfp}}\frac{\nu^4}{\mathscr{I}(\nu)}, \quad \text{(A9)}$$

versus the idealization of Equation (10) that

$$\lambda_{\mathrm{approx}}(\nu) = \frac{4}{15}\lambda_{\mathrm{mfp}}\nu^4 = 0.2666\lambda_{\mathrm{mfp}}\nu^4. \quad \text{(A10)}$$

In the regime where Equation (A8) is appropriate, Equation (A9) reduces to become

$$\lambda_{\mathrm{accurate}}(\nu \gg 1) \simeq \frac{2}{3}0.3770\lambda_{\mathrm{mfp}}\nu^4 = 0.2513\lambda_{\mathrm{mfp}}\nu^4, \quad \text{(A11)}$$

which is less than $\simeq$5% away from the form being used in the text. Note that it is in this regime that K_e^* is determined at $\nu_q = 3.75$, so the errors in using the approximate form do not seriously modify the estimate where SB transport lapses. However, we do use the full speed dependence of the free path to get the proper extensions of the $\nu_2(K_e)$ blue curve in Figure 1(a).

APPENDIX B

VARIATION OF β ACROSS MAIN-SEQUENCE STARS

The solar normalized luminosity, $L/L_\odot$, and mass, $M/M_\odot$, of MS stars are empirically related (Lang 1992) by

$$\frac{L}{L_\odot} \simeq \left(\frac{M}{M_\odot}\right)^{3.8}. \quad \text{(B1)}$$

Together with the Stefan–Boltzmann Law, Equation (B1) implies that

$$\frac{T}{T_\odot} = \left(\frac{M}{M_\odot}\right)^{0.95}\left(\frac{R_\odot}{R}\right)^{1/2}, \quad \text{(B2)}$$

which implies that the ratio of the squares of the escape speed to the acoustic speed becomes

$$\beta = \beta_\odot\left(\frac{M}{M_\odot}\right)^{0.05}\left(\frac{R_\odot}{R}\right)^{1/2}. \quad \text{(B3)}$$

Using MS star data (Schmidt-Kaler 1982), β varies only by factors of four on either side of the solar value, $\beta_\odot = 1925$ for a range of MS stars; this variation determines Figure 4.

REFERENCES

Braginskii, S. I. 1965, RvPP, 1, 205
Bray, R. J., Cram, L. E., Durrant, C., & Loughhead, R. E. (ed.) 2006, Plasma Loops in the Solar Corona (Cambridge: Cambridge Univ. Press)
Chandran, B. D. G., Dennis, T. J., Quataert, E., & Bale, S. D. 2011, ApJ, 743, 197
Cranmer, S. R., van Ballegooijen, A. A., & Edgar, R. J. 2007, ApJS, 171, 520
Dorelli, J. C., & Scudder, J. D. 1999, GeoRL, 26, 3537
Dorelli, J. C., & Scudder, J. D. 2003, JGR, 108, 1294
Dreicer, H. 1959, PhRv, 115, 238
Dreicer, H. 1960, PhRv, 117, 329
Dzifcáková, E., Homola, M., & Dudík, J. 2011, A&A, 531, A111
Esser, R., & Edgar, R. J. 2000, ApJL, 532, L71
Feldman, W. C., Asbridge, J. R., Bame, S. J., Montgomery, M. D., & Gary, S. P. 1975, JGR, 80, 4181
Fontenla, J. M., Avrett, E. H., & Loeser, R. 1990, ApJ, 355, 700
Fuchs, V., Cairns, R. A., Lashmore-Davies, C. N., & Shoucri, M. M. 1986, PhFl, 29, 2931
Grad, H. 1949, Commun. Pure Appl. Math., 2, 331
Gray, D. R., & Kilkenny, J. D. 1980, PlPh, 22, 81
Gurevich, A. V., & Istomin, Y. N. 1979, JETP, 50, 470
Hazeltine, R. D., & Waelbroeck, F. L. 2004, The Framework of Plasma Physics, Frontiers in Physics (New York: Perseus Books)
Hollweg, J. V. 1974, JGR, 79, 3845
Ko, Y.-K., Fisk, L. A., Gloeckler, G., & Geiss, J. 1996, GeoRL, 23, 2785
Landi, S., & Pantellini, F. G. E. 2001, A&A, 372, 686
Lang, K. R. 1992, Astrophysical Data: Planets and Stars (Berlin: Springer)
Leblanc, F., & Hubert, D. 1998, ApJ, 501, 375
Lee, E., Williams, F. R., & Lapenta, G. 2013, A&A, in press (arXiv:1305.2939)
Montgomery, D., Turner, L., & Joyce, G. 1974, PhFl, 17, 954
Olbert, S. 1968, in Physics of the Magnetosphere, ed. R. D. L. Carovillano & J. F. McClay (Astrophysics and Space Science Library, Vol. 10; Dordrecht: Reidel), 641
Olbert, S. 1983, in Solar Wind 5 NASA Conf. Proc., CP-2280, ed. M. Neugebauer (Washington, DC: NASA STI), 149
Pannekoek, A. 1922, BAN, 1, 107
Pierrard, V. 2010, SoPh, 267, 153
Pinfield, D. J., Keenan, F. P., Mathioudakis, M., et al. 1999, ApJ, 527, 1000
Rosseland, S. 1924, MNRAS, 84, 720
Schmidt-Kaler, T. 1982, in Stars and Star Clusters, ed. K. Schaifers (Berlin: Springer)
Scudder, J. D. 1992, ApJ, 398, 319
Scudder, J. D. 1996a, JGR, 101, 13461
Scudder, J. D. 1996b, JGR, 101, 11039
Scudder, J. D., & Olbert, S. 1979, JGR, 84, 2755
Scudder, J. D., & Olbert, S. 1983, Solar Wind 5 NASA Conf. Proc., CP-2280, 163
Shoub, E. C. 1983, ApJ, 266, 339
Spitzer, L. 1962, Physics of Fully Ionized Gases (New York: Wiley), 139
Tanenbaum, B. S. 1967, Plasma Physics (New York: McGraw-Hill)
Wilhelm, K., Marsch, E., Dwivedi, B. N., et al. 1998, ApJ, 500, 1023